Microbial survival strategies in biological soil crusts of polymetallic tailing wetlands

Zekai Feng, Guobao Wang, Yuanyuan Jiang, Chiyu Chen, Daijie Chen, Mengyao Li, Jean Louis Morel, Hang Yu, Yuanqing Chao, Yetao Tang, et al.

Microbial survival strategies in biological soil crusts of polymetallic tailing wetlands

Zekai Feng [a], Guobao Wang [a,b,*], Yuanyuan Jiang [a], Chiyu Chen [a], Daijie Chen [a], Mengyao Li [a], Jean Louis Morel [c], Hang Yu [a], Yuanqing Chao [a,b], Yetao Tang [a,b], Rongliang Qiu [a,d,e], Shizhong Wang [a,b,*]

[a] School of Environmental Science and Engineering, Sun Yat-sen University, Guangzhou 510006, China
[b] Guangdong Provincial Key Laboratory for Environmental Pollution Control and Remediation Technology, Sun Yat-sen University, Guangzhou 510006, China
[c] Laboratoire Sols et Environnement, UMR 1120, Université de Lorraine, INRAE, Vandoeuvre-lès-Nancy 54518, France
[d] Guangdong Laboratory for Lingnan Modern Agriculture, Guangzhou 510642, China
[e] Guangdong Provincial Key Laboratory of Agricultural & Rural Pollution Abatement and Environmental Safety, College of Natural Resources and Environment, South China Agricultural University, Guangzhou 510642, China

ARTICLE INFO

ABSTRACT

The role of biological soil crusts (biocrusts) in ecological restoration is dominated by microbiota. This has been extensively studied in arid ecosystems characterized by nutrient deficiencies and poor soil substrates, including metal(loid)-rich mining regions. However, in the prior study areas, water constraints obscured the toxicity and restriction of succession by heavy metals, which were essential for soil remediation in mining regions using biocrusts. Accordingly, in the current study, we characterized biocrusts from a typical polymetallic tailing wetland and performed pot incubation to evaluate microbial community succession and microbial co-occurrence patterns. Results showed that adequate water and heavy-metal stress produced thicker and more hydrophobic biocrusts than did arid conditions, promoting stronger microbial activity in tailing wetlands. Moreover, the bioinformatic analyses during pot incubation suggest three potential survival strategies. (1) *Cyanobacteria* variation improved the succession level of cyanobacterial crusts. Even under heavy-metal stress, succession from light to dark cyanobacterial crusts still occurred, with *Coleofasciculaceae* decreasing 63% and *Scytonema* increasing 59% compared with the control groups. (2) Keystone taxa variation maintained high inorganic nitrogen turnover. Organisms potentially capable of inorganic nitrogen turnover, including *Chloroflexi* A4b and SBR1031, maintained a high relative abundance accounting for 42% (15/36) of the keystone taxa. (3) Variations in the interactions among microbiota created closer-knit microbial networks. Compared with the control groups, fewer nodes (15.2%) maintained higher average clustering coefficient values (1.8%) through 14% more positive interactions in the groups exposed to heavy-metal stress at the end of the incubation experiment. This study provides insights into the distinctive survival strategies of biocrusts in metal-rich extreme environments, offering theoretical support for biocrust-mediated ecological restoration in humid metal-contaminated regions.

1. Introduction

Promoting biodiversity and biological function in disturbed soil ecosystems is an important aspect of ecological restoration in extreme environments (Bardgett and van der Putten, 2014). Soil microorganisms have attracted increasing attention in this field (Calderón et al., 2017) due to their essential roles in elemental biogeochemical cycling and their ability to thrive in high-stress conditions (Falkowski et al., 2008;

Ciccazzo et al., 2016; Venter et al., 2018). One exemplary group of organisms is the biological soil crusts (biocrusts). Acting as pioneer communities in extreme environments, biocrusts form intimate associations between soil particles with both photoautotrophic (*e.g.,* cyanobacteria, algae, lichens, bryophytes) and heterotrophic (*e.g.,* bacteria, fungi, archaea) organisms (Weber et al., 2022). These 'ecological engineers' play an indispensable role in ecological restoration in nutrient cycling, water conservation, and soil stabilization within arid and semi-arid

---

regions (Belnap, 2003a; Rodriguez-Caballero et al., 2018).

Biocrusts have been discovered in metal(loid)-rich mining regions (Huang et al., 2011; Liu et al., 2012; Nyenda et al., 2019; Guo et al., 2022), where they improve C/N content and promote vegetation colonization (Ye et al., 2002). However, the mining regions, known for their barren and extreme environments (Nyenda et al., 2019; Xiao et al., 2022), also impose challenges due to the detrimental impact of heavy metals on the structure, diversity, and co-occurrence patterns of microbial communities (Gauthier et al., 2014; Sun et al., 2020b; Chun et al., 2021). Recruitment of phototrophic microorganisms, such as *Cyanobacteria*, and chemolithotrophic participants, including *Thiobacillus*, is a crucial mechanism by which microbial communities respond to heavy-metal stress (Mendez et al., 2008; Chung et al., 2019), attributed to nutrient accumulation processes (Sun et al., 2018). However, as a predominant microbial constituent in biocrusts, abundant *Cyanobacteria* is associated with enriched nutrient elements and an increased abundance of copiotrophic microorganisms compared to tailing sand without biocrusts cover (Weber et al., 2015). Thus, compared to the prevailing focus on nitrogen input, the turnover of inorganic nitrogen might represent a key mechanism for efficient microbial nitrogen utilization within biocrusts (Nelson et al., 2016). This requires cooperation among various microorganisms with distinct metabolic pathways; biocrusts provide an ideal habitat for such symbiotic relationships (Kuypers et al., 2018; Kratz et al., 2022). Consequently, the complexity of nitrogen cycling and microbial interactions in biocrusts, compared to tailing sand, might confer distinctive survival strategies in response to heavy-metal stress. However, the influence of heavy metals on microbiota during early ecological succession in biocrusts and the microbial survival strategies under heavy-metal stress remain largely unknown. Understanding these interactions is vital for establishing effective ecological restoration strategies in metal-contaminated mining regions, enabling targeted approaches to enhance restoration efforts and facilitate vegetation (Guo et al., 2022).

Moreover, most prior studies have focused on biocrusts in arid and semi-arid regions, where water is the limiting factor for microbial activity (Zhao et al., 2021). Hence, a predominant focus is often directed toward examining biocrust responses to varying precipitation conditions and water cycling (Swenson et al., 2018; Tamm et al., 2018; Deng et al., 2020; Maier et al., 2021), potentially overshadowing the exploration of biocrust survival strategies under heavy-metal stress. Furthermore, this aspect has not been investigated within the limited studies reporting on biocrusts in humid regions (Thomas et al., 2006; Wang et al., 2022a; Wang et al., 2023).

Meanwhile, biocrusts were identified in a downstream wetland adjacent to a well-remediated poly-metal tailing pond in South China. These biocrusts are well hydrated and coexist with heavy metal(loid)s. Thus, the current study characterized these biocrusts and performed indoor pot incubation combined with bioinformatic analysis to confirm the influence of adequate water and heavy metals, and to characterize biocrust survival strategies following the application of severe heavy-metal stress. The objectives of this study were to (1) characterize the morphology, structure, and microbial community composition of tailing wetland biocrusts in the field under sufficient water and heavy-metal stress; (2) describe the microbial community succession and co-occurrence patterns under heavy-metal stress in the absence of water as the primary limiting factor in indoor pot incubations; (3) hypothesize biocrust survival strategies in tailing wetlands. Our findings provide important insights into the development of effective ecological restoration strategies in metal-contaminated mining regions.

2. Materials and methods

2.1. Study area and sampling

Biocrusts were collected in December 2021 from a tailing wetland downstream of an abandoned polymetallic tailing pond (24°22′55″N,116°12′49″E) in Meizhou, Guangdong Province, China (Wang et al., 2020a; Wang et al., 2020b). The annual mean temperature is 21.3 °C and the mean precipitation is 1620 mm. The tailing pond, abandoned in 1992, was destroyed by Typhoon "Suli" in July 2013, releasing tens of thousands of tons of tailing sand into the downstream reservoir area (Liang et al., 2017), in which a tailing wetland emerged subsequently. To address the metal(loid) pollution in the downstream wetland, comprehensive re-greening efforts were undertaken for the tailing pond. Common plants, including *Cynodon dactylon* L., *Hibiscus cannabinus* L., and *Nerium indicum Mill*, were successfully planted with organic amendment (Wang et al., 2020b). Accordingly, the heavy metal content in the mine drainage flowing into the wetland is relatively low (Table S2), leading to rapid primary succession in the wetland. After four years of succession, most of the wetland surface was covered with biocrusts. A total of 12 biocrusts (10 × 10 cm) were collected (four groups were collected in triplicate; detailed group sets are described in Subsection 2.2). The sampling sites were carefully selected to ensure that no plants had grown. The biocrusts remained in contact with water throughout the year; during the rainy season, the water surface in this stream bank typically reached the upper surface of the biocrusts. The wetland substrate (bare tailing sand without biocrusts cover) was also sampled nearby. Detailed sampling methods and photos of the sampling sites are shown in Figs. S1, S2, and Text S1.

2.2. Experimental design

An indoor pot study was conducted using a factorial design to accentuate microbial survival strategies in biocrusts under more severe heavy-metal stress and to assess the limited influence of water on microbial community structure under sufficient moisture. The factors used in this study included: (i) heavy-metal stress (group C, control group without heavy-metal stress and group T, treatment group with 5 mg L^{-1} Zn and 10 mg L^{-1}Cd), (ii) water conditions (simulated wetlands for dry (group D) and wet seasons (group W)), and (iii) incubation time (day 0, day 40, and day 100). The control wetland (C) served as a representative low-pollution environment similar to the study area. Meanwhile, the treatment wetland (T) with Zn and Cd stress was designed to create a simulated tailing wetland, providing insights into the survival strategies of biocrusts under high-stress conditions. Additionally, the water levels during the wet (W) and dry (D) seasons, which exhibited the largest difference in precipitation, were simulated to highlight the influence of water on microbial communities.

All simulated wetlands, established in plastic basins (15 × 15 × 15 cm), utilized silica as the substrate (1.8 kg per basin). However, the sand in the group T was supplemented with additional CdCl$_2$ and ZnCl$_2$ to simulate heavy-metal stress. The metal-polluted sand was thoroughly mixed to ensure even distribution of the metals before the incubation. During the dry-season simulation, water was flooded over the substrate to ensure that the biocrusts remained in constant contact with water, while during the wet season, the water surface was level with the biocrust upper surface. The incubation period spanned 100 days, during which biocrust samples were collected on days 0, 40, and 100. Samples collected on day 0 represented biocrusts under original field conditions, labeled IN (inoculant). All incubations occurred in a greenhouse under 1500 lx illumination (12 h light; 25 °C/12 h dark; 20 °C). The relative humidity was maintained at 60 %. Biocrusts were watered daily. Each treatment was performed in triplicate. Group sets are also shown in Fig. S3.

2.3. Physicochemical analyses

Freeze-dried samples from the IN group (initial samples before incubation) were investigated. In addition to whole biocrusts, the properties of their upper (UBSC) and lower (LBSC) layers (stratification shown in Subsection 3.1), and bare tailing sand were also analyzed. Morphologies and microstructures were characterized using

stereomicroscopy (Leica S9I, Germany) and field emission scanning electron microscopy (SEM) (Gemini 500, Zeiss/Bruker, Germany), coupled with energy-dispersive X-ray spectroscopy (EDS). The vertical distributions of biocrust elements were determined using micro X-ray fluorescence (μ-XRF) (M4TORNADO, Bruker, Germany). Soil water repellency (SWR) was measured by the standard water drop penetration time (WDPT) test (Mugnai et al., 2018). Measurements were divided into hydrophilic (0–1 s), non-water repellent (1–5 s), slightly water repellent (5–60 s), and strongly water repellent (60–600 s). Both pH and Eh were measured using a pH-Eh meter (SANXIN, China). Total organic carbon (TOC) content was measured according to a method adapted from Mingorance et al. (2007). Total nitrogen (TN) and total carbon (TC) were measured using an elemental analyzer (Vario EL Cube, Elementar, Germany). Chlorophyll was measured using the method of Caesar et al. (2018), while polysaccharides were quantified followed the procedure described by Huang et al. (2021). The metal(loid) content of the biocrusts was assessed through inductively coupled plasma optical emission spectrometry (ICP-OES) (PerkinElmer, Avio 500, USA) after digested by microwave digestion (MARS6, USA).

Further analyses were performed on the biocrusts incubated indoor at three time points (*i.e.,* days 0, 40, and 100). Potentially bioavailable fractions of metal(loid)s were extracted using 0.3 mol/L HNO_3 (Brady et al., 2016) and measured by ICP-OES. Standard reference materials (*e. g.,* GBW07405) and reagent blanks were used for quality control. Detailed operations and methods for determining the SWR, TOC, and potentially bioavailable fractions of metal(loid)s are provided in Text S2.

2.4. DNA extraction, 16S rRNA gene amplification, sequencing, and bioinformatic analyses

DNA was extracted using the FastDNA® SPIN Kit for Soil (MP Biomedicals, France) according to the manufacturer's protocol. DNA concentration and quality were confirmed by spectrophotometry using a NanoDrop 2000 spectrophotometer (Thermo Fisher Scientific, USA). The V3-V4 hypervariable region of the 16S rRNA gene was amplified using barcoded primers 338F (5′-ACTCCTACGGGAGGCAGCAG-3′) and 806R (5′-GGACTACHVGGGTWTCTAAT-3′). Amplicons were sequenced on the Illumina HiSeq 2500 PE250 platform (Biomarker Technologies Corporation, Beijing, China) (Miya et al., 2015). Paired-end reads were overlapped, merged, and pre-processed using the QIIME2 pipeline (2020.2) (Bolyen et al., 2019). Amplicon sequence variants (ASVs) were merged into a feature table that concentrated representative reads for further analyses. Species annotation was performed using the silva-138–99-515–806-nb-classifier in QIIME2 (Quast et al., 2012; Yilmaz et al., 2014).

2.5. Statistical analyses

Repeated measures analysis of variance (RM-ANOVA) was employed to investigate the effects of heavy-metal stress, water conditions, incubation time, and their interactions on biocrust indicators. The Tukey honestly significant difference (HSD) post-hoc test for one-way analysis of variance (ANOVA) was used to identify differences and significance in various biocrust indicators during incubation. Alpha (α) diversity indices, including Chao1 and Simpson, and beta (β) diversity values based on Weighted UniFrac distance were calculated in QIIME2 using the "q2-phylogeny" pipeline. The β-diversity of principle coordination analysis (PCoA) was used to assess community structure variation. Venn diagrams were produced online (https://jvenn.toulouse.inra.fr/app/index.html) (Bardou et al., 2014). Microbial co-occurrence networks were analyzed based on an online pipeline (https://ieg4.rccc.ou.edu/mena) (Zhou et al., 2010; Zhou et al., 2011) and visualized using 'Gephi' software (v0.9.2) (Bastian et al., 2009). Pearson correlation analysis was used to identify pairwise correlation in co-occurrence networks. Robustness and cohesion indices were evaluated to assess the stability of

microbial co-occurrence networks using the R scripts adapted from Yuan et al. (2021) and Herren and McMahon (2017), respectively. Random forest (RF) analysis was used to predict the contribution of keystone taxa to microbial network stability (Cutler et al., 2007; Jiao et al., 2018), using the R package 'randomForest'. Detailed information on the co-occurrence networks, identification methods for keystone taxa, and the calculation methods for robustness, cohesion, and RF analysis are provided in Text S3.

3. Results

3.1. Characteristics of biocrusts in tailing wetlands

As shown in Table 1 and Table S2, the metal(loid) concentrations in mine drainage were notably lower than those reported in previous studies, comparable to those after bioremediation (Bwapwa et al., 2017). pH values in biocrusts and mine drainage exceeded 7.5, considering the effect of pH on the bioavailability of metal(loid) ions, the study area can be assigned a low pollution status.

The morphologies and microstructures of biocrusts under field conditions (incubation day 0, group IN) are shown in Fig. 1. Biocrusts exhibited a smooth surface, a mean thickness of approximately 1 cm, and two distinct layers of stratification (Fig. 1a). The UBSC was dense, whereas the LBSC appeared to be sandy soil (Fig. 1b). The vertical distribution of the elements also varied between layers (Fig. 1d, Table 1). Moreover, microbes, including green algae, were tightly bound to mineral particles (Fig. 1c). SEM micrographs also showed a similar phenomenon, in which mineral particles were held together by filaments with carbon and sulfur enrichments (Fig. 1e); these may be biomass, such as mycelium or extracellular polymeric substances (EPS) produced by the microorganisms. In the case of enriched metal(loid)s (*e. g.,* As, Cd, and Zn) (Table 1), the TC and TN in biocrusts were 3.3- and 8.7-fold higher than in tailing sand, respectively. Biocrust chlorophyll content was also significantly higher than in tailing sand, indicating the presence of photosynthetic microorganisms. Biotic and abiotic components tightly bound in biocrusts produced stronger soil water repellency, a common feature of biocrusts (Yang et al., 2014; Keck et al., 2016), which likely reduced soil erosion in mine tailings.

In summary, biocrusts successfully colonized the tailing wetland and demonstrated a robust ability to fix carbon and nitrogen.

3.2. Physicochemical properties of biocrusts during incubation

During pot incubation, variations were observed in basic physicochemical properties, including pH, essential nutrients (*e.g.,* carbon, nitrogen, and phosphorus), and heavy metals (Fig. 2). To better demonstrate these variations during incubation, samples from different groups were combined together when no significant effects of heavy metals or water conditions were observed based on RM-ANOVA (Fig. 2, Tables S5–S10). Throughout the incubation period, RM-ANOVA showed that incubation time was the only factor that significantly impacted the pH (Table S5). Thus, the pH gradually increased from 7.96 to 8.13 in group T and 8.43 in group C, with no significant difference observed between the two groups on day 100 (Fig. 2a). Meanwhile, the concentration of heavy metals (*i.e.,* Cd and Zn) in the biocrust of group T reached an approximate equilibrium on day 40, with 830 % (Cd) and 30 % (Zn) increases compared to the IN group (Fig. 2b, c).

The RM-ANOVA results also indicated that heavy metals had no significant effect on biocrust TC or TN, while water conditions significantly impacted TN. TC, on the other hand, was primarily influenced by the interaction effects between incubation time and water, as well as between incubation time and heavy-metal stress. The TN in group W (0.14 %) was 27 % higher than in group D (0.11 %) on day 100. Similarly, the TC was 41 % higher in group W (2.33 %) than in group D (1.65 %) on day 100, although significant differences were not observed between days 100 and 0 (Fig. 2e, f). Notably, neither the water conditions

Table 1
Basic physicochemical properties of biocrusts of different layers and the bare tailing sand under field conditions

Sample[a]	Heavy metal(loid)s (g kg^{-1})						pH	Eh (mV)
	As	Cd	Zn	Pb	Fe	Mn		
TS[b]	2.67 ± 0.43a	0.08 ± 0.01a	2.96 ± 0.54a	1.66 ± 0.27a	22.0 ± 5.0a	5.10 ± 1.1ab	8.37 ± 0.07a	210 ± 2.9a
BSC[c]	2.14 ± 0.59b	0.04 ± 0.01b	2.60 ± 0.32ab	1.05 ± 0.20b	24.9 ± 7.0a	6.40 ± 3.4ab	7.99 ± 0.34b	149 ± 16.0b
UBSC[d]	1.10 ± 0.02c	0.02 ± 0.00c	2.20 ± 0.45ab	0.52 ± 0.01c	22.3 ± 2.2a	6.80 ± 0.6a	7.90 ± 0.03b	148 ± 17.7b
LBSC[e]	1.80 ± 0.15bc	0.02 ± 0.00c	2.00 ± 0.24b	1.10 ± 0.01b	20.4 ± 1.6a	4.60 ± 0.4b	7.90 ± 0.10b	123 ± 3.3c

Sample	TOC %	TC %	TN %	Chlorophyll (mg m^{-2})	Chlorophyll (mg kg^{-1})	WDPT(s)[f]	Polysaccharide (mg kg^{-1})
TS	0.60 ± 0.05d	0.59 ± 0.02c	0.07 ± 0.00c	—	0.43 ± 0.40d	0c	5.35 ± 0.36d
BSC	1.50 ± 0.40b	1.94 ± 0.10b	0.61 ± 0.04b	240 ± 20.8a	21.4 ± 1.49b	53.9 ± 32.83b	35.0 ± 7.28b
UBSC	3.67 ± 0.13a	5.41 ± 1.00a	0.33 ± 0.06a	213 ± 24.8a	76.7 ± 10.30a	53.9 ± 32.83b	97.7 ± 5.76a
LBSC	0.86 ± 0.05c	0.92 ± 0.06bc	0.29 ± 0.02bc	4.84 ± 4.2b	0.94 ± 0.74c	10.7 ± 1.24	8.58 ± 1.03c

[a] All data in this table displays the characteristics of the samples taken from the original tailing wetland.
[b] TS means the bare tailing sand.
[c] BSC means biological soil crust.
[d] UBSC means the upper layer of the BSC.
[e] LBSC means the lower layer of the BSC.
[f] WDPT is the standard water drop penetration time to reflect soil water repellency.
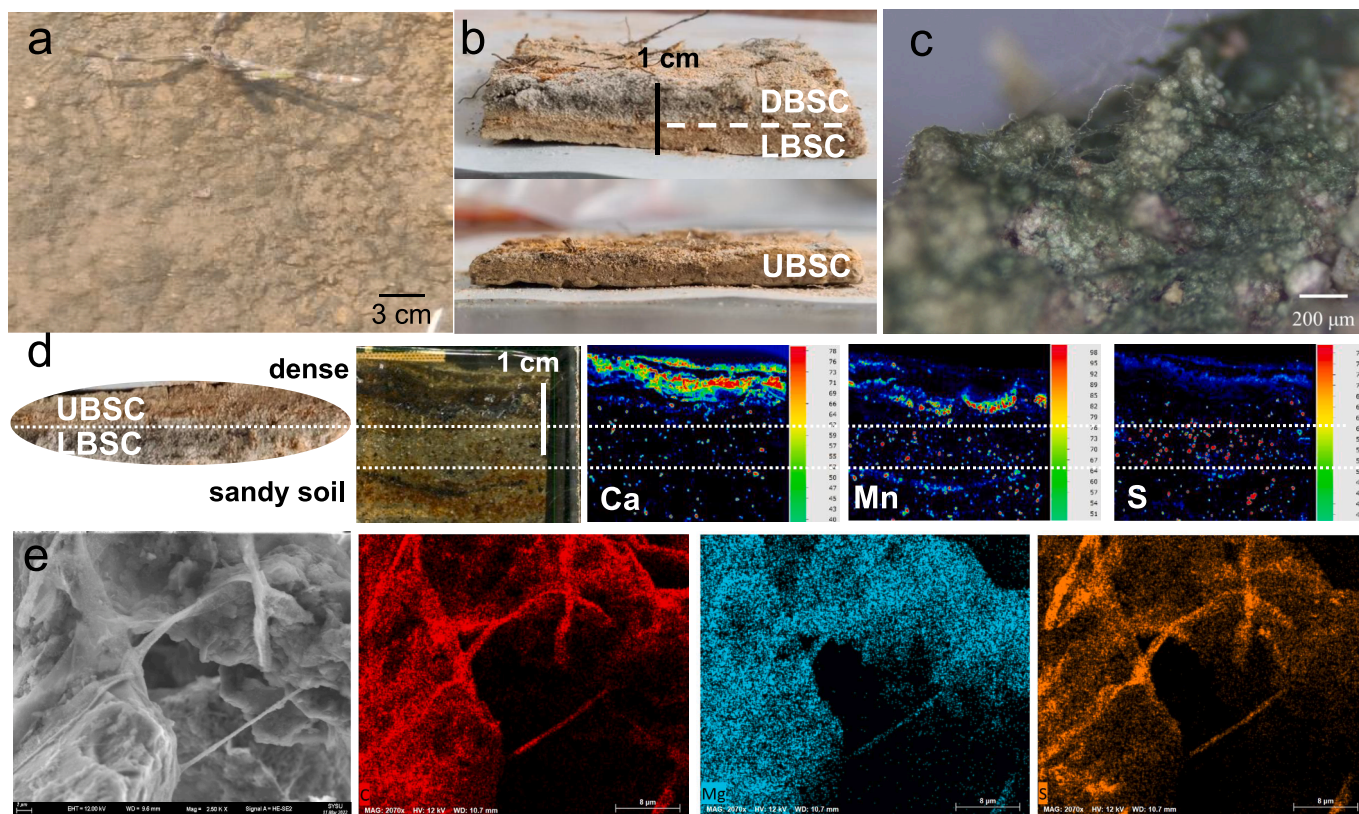

Fig. 1. Morphology, microstructure, and elemental mappings of biocrusts. (a) Morphology of biocrusts under field conditions. (b) Apparent stratification of biocrusts. (c) Tight binding of mineral particles and microorganisms in the upper layer of the biocrusts. (d) Vertical distribution of elements in biocrusts. (e) SEM image and EDS elemental mappings of biocrusts. UBSC represents the upper layer of the biocrusts, and LBSC represents the lower layer of the biocrusts.

nor heavy metals significantly impacted phosphorus content (Fig. 2d, S4, Table S8).

In summary, biocrusts accumulated large amounts of heavy metals in group T. However, extreme heavy-metal stress did not significantly impact pH or C/N accumulation, suggesting that biocrusts are resistant to heavy-metal stress.

3.3. Microbial community succession

In 16S rRNA gene sequencing, 23,545 ASVs were obtained. Based on RM-ANOVA results, while microbial α-diversity was significantly affected by heavy-metal stress, water conditions had a limited impact on it (Tables S11, S12). Both Chao1 and Simpson indices reached their lowest values in the group T, and were significantly lower than those in the group C (Fig. 3a). Besides, PCoA and permutational multivariate analysis of variance (PerMANOVA) test also revealed significant differences in the microbial community structure among groups under various heavy-metal stresses (Fig. 3b, Tables S3, S4, and S13). In contrast, no significant differences were observed among groups subjected to different water conditions.

For a more comprehensive depiction of the effects of heavy metals and water conditions on community structure, Venn diagrams were
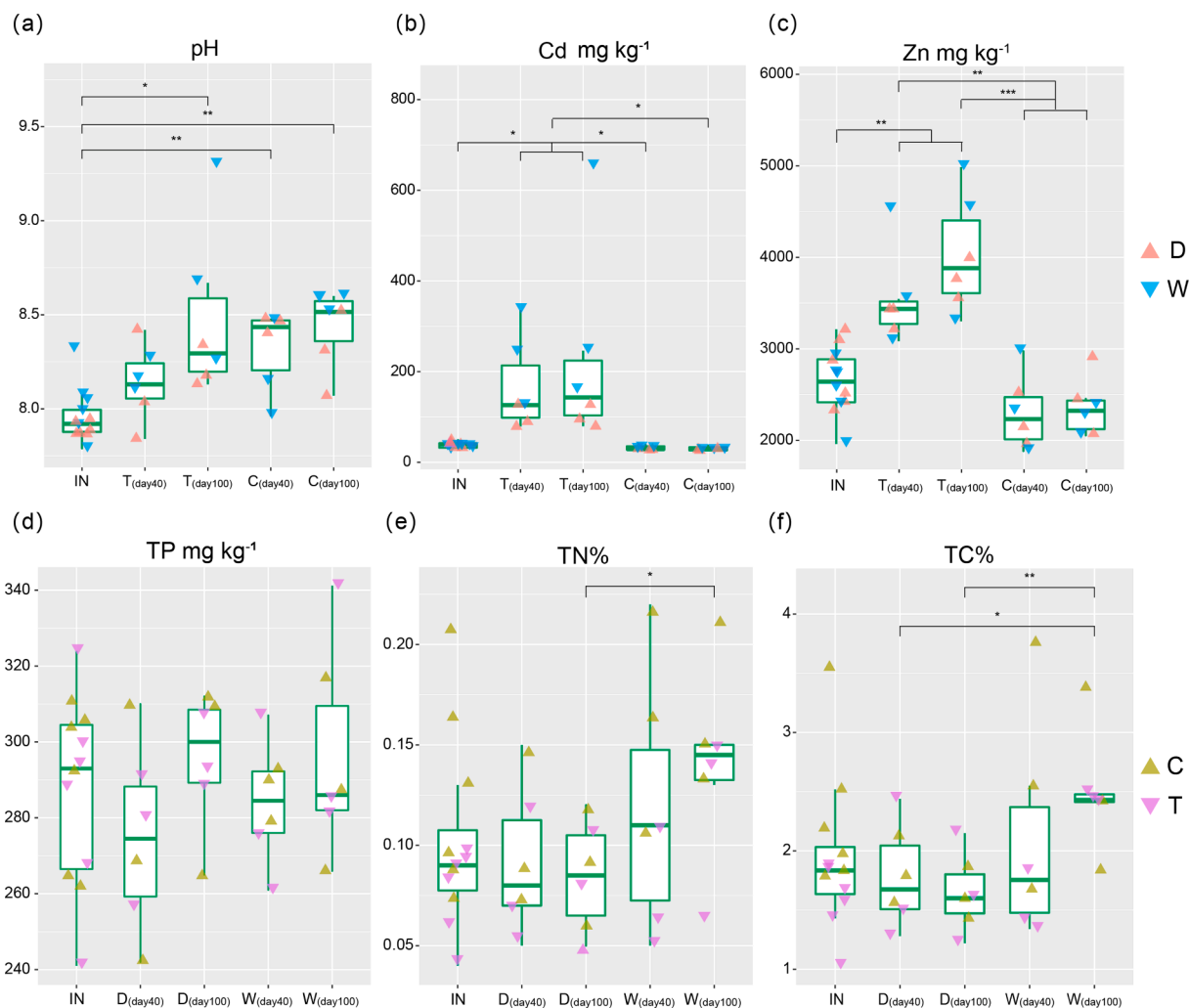
Fig. 2. Ph, nutrient concentrations (*i.e.,* TN, TC, and TP), and heavy metal contents (*i.e.,* Cd and Zn) in studied samples. Variations in pH (a), Cd (b), and Zn (c) between the treatment and control groups and the influence of water conditions on the TP (d), TN (e), and TC (f) between the wet and dry groups during incubation. IN means the initial condition of biocrusts at the beginning of the incubation, T and C represent groups with and without heavy-metal stress, respectively, and D and W represent groups under dry and wet water conditions, respectively.

generated (Fig. 3c, d) and redundancy analysis (RDA) was performed (Fig. S7). Biocrusts in groups D and W shared 27 % and 55 % more ASVs than groups C and T on days 40 and 100, respectively. Moreover, groups C and T were readily divided by the x-axis via the RDA. These data further support the notion that water conditions exert limited influence on microbial communities.

A comprehensive microbial community succession was observed based on variations at the phylum and genus levels. (Fig. 4). *Chloroflexi*, *Cyanobacteria*, and *Proteobacteria* were the dominant phyla across all groups (Fig. 4a). By day 100, minimal variation was observed in *Chloroflexi* among all groups. In contrast, *Cyanobacteria* were 34 % more abundant in group T, while *Proteobacteria* demonstrated a 25 % enrichment in group C. The heatmap (Fig. 4b) showing the 10 most abundant ASVs in each group illustrates the detailed succession. Notably, the stable overall abundance of *Chloroflexi* might be attributed to the contrasting distribution trends among its genera. For example, ASV5 (A4b), ASV7 (A4b), ASV10 (*uncultured Chloroflexi*), and ASV19 (A4b) were enriched in group C, while ASV4 (A4b), ASV9 (JG30-KF-CM45), ASV15 (A4b), and ASV17 (JG30-KF-CM45) were enriched in group T. Meanwhile, the distribution of *Cyanobacteria* might be due to ASV1, 2, and 3 (*Scytonema*) maintaining high relative abundances in group T. Between groups D and W, differences were only observed for *Nitrospirota* (1.4 %) in group C (*P* = 0.050) and *Planctomycetota* (3.3 %)

in group T (*P* < 0.05). This is consistent with the limited influence of water on microbial community structure.

3.4. Network interactions and keystone taxa

Interaction variability is often regarded as a key regulator of microbial community succession dynamics (Qiu et al., 2021). Thus, microbial co-occurrence networks were established to reveal variations during incubation (Fig. 5a–e). To meet the computational requirements for co-occurrence networks when considering the limited impact of water conditions and the apparent influence of heavy metals, we restricted our analysis to groups IN, T, and C networks. The detailed node and edge attributes in each co-occurrence network and the topological properties calculated by the online pipeline are provided in Tables 2 and S14–23. In detail, the numbers of nodes and edges and modularity of the small-world coefficient σ in group C were all higher than those in group T, indicating that the negative influence of heavy metals made networks in group T more fragile and less efficient (Yuan et al., 2021a; Yuan et al., 2021b). However, the average clustering coefficient (avgCC) in group T was 1.8–3.7 % higher than in group C. On day 100, 14 % more positive interactions were found in group T, indicating a closer and interspecific cooperative relationship among microbiota under heavy-metal stress (Barberán et al., 2012). Notably,
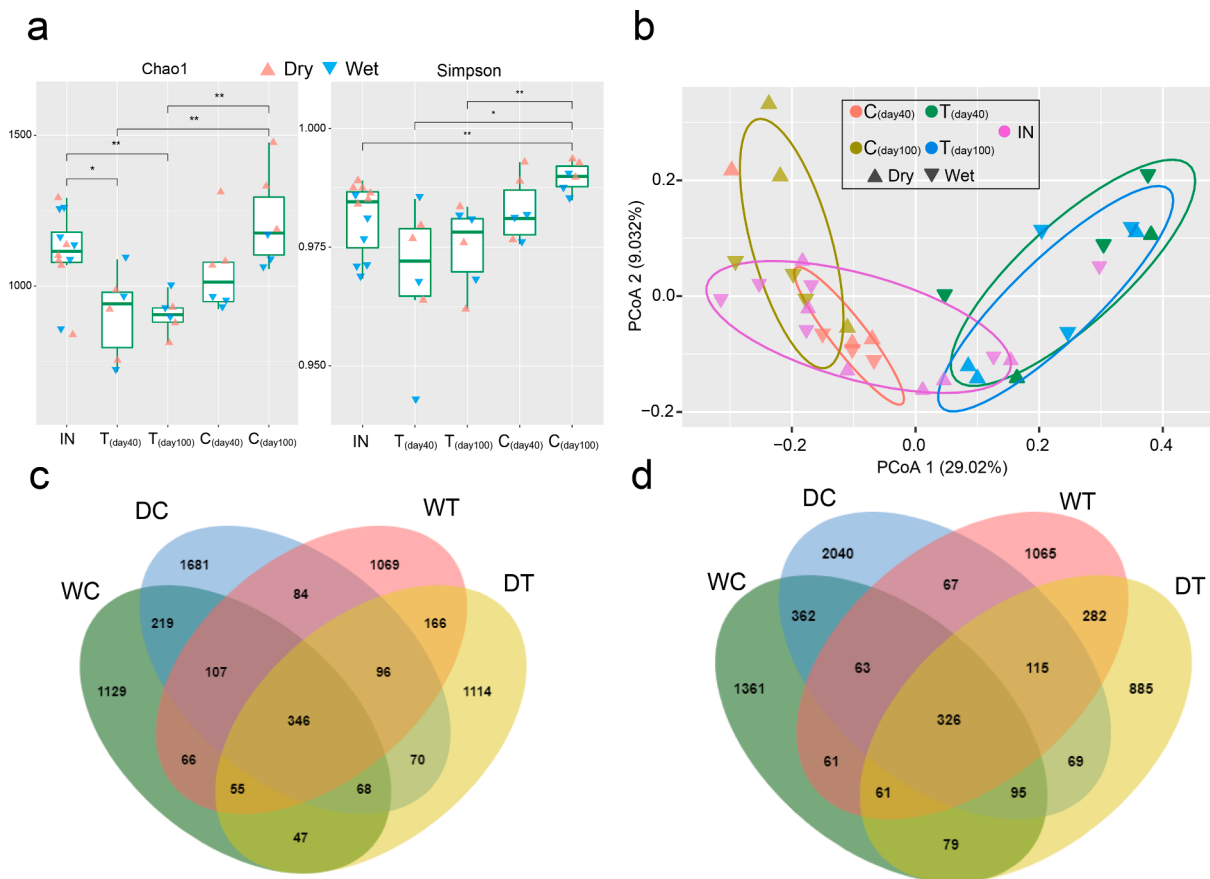
Fig. 3. Microbial community diversity and composition of biocrusts during incubation. (a) Alpha diversity indices. (b) Principal coordinate analysis (PCoA) based on the Weighted UniFrac distance. The ellipse represents the 68% confidence interval. Venn diagram showing unique and shared ASVs at day 40 (c) and day 100 (d). IN means the initial condition of biocrusts at the beginning of the incubation, T and C represent groups with and without heavy-metal stress, respectively, and D and W represent groups under dry and wet water conditions, respectively.

the topological properties in group T gradually converged with those of group C during incubation, suggesting that the microbiota gradually adapted to the environment to form a more stable network. This further suggests that microbiota in biocrusts vary their co-occurrence patterns to survive under heavy-metal stress.

Keystone taxa were identified through network analysis (*i.e.,* module hubs and connectors) (Fig. 5f) (Liu et al., 2022). During incubation, they varied (Table S1), with only ASV49 (SBR1031) and ASV92 (A0839) present in multiple groups. However, their potential functions remained largely unchanged, excluding group T on day 100. Specifically, inorganic nitrogen-cycling-associated microorganisms accounted for 48 % of keystone taxa and were present in all other groups. However, in group T, on day 100 microorganisms crucial for EPS production and microbial biofilm formation became keystone taxa (*e.g.,* ASV92 A0839 and ASV438 *Sandarakinorhabdus*) (Cydzik-Kwiatkowska, 2015; Di Gregorio et al., 2017), suggesting the importance of these functions under chronic heavy-metal stress.

3.5. Impact of keystone taxa on the community stability

To assess how environmental stress affects microbial co-occurrence patterns, we selected cohesion and robustness indices to evaluate network stability (Hernandez et al., 2021). Positive and negative cohesion reflect the degree of cooperative behaviors and competitive interactions among community members, respectively (Herren and McMahon, 2017; Yuan et al., 2021a). Thus, the negative-to-positive cohesion ratio (negative: positive cohesion) was used to predict the stability of co-occurrence networks (Hernandez et al., 2021). On day 40,

group T had the lowest ratio (0.707), while group C had the highest (0.836) (Fig. 6a). Robustness exhibited similar patterns (Fig. 6b, S8); on day 40, group T exhibited a significantly lower value (0.414) than group C on day 100 (0.419). These indices demonstrate that heavy metals reduce community stability while affecting community composition, particularly on day 40. Notably, significant differences in the negative: positive cohesion were not observed between groups C and T on day 100, suggesting attempts by the microbiota to adapt to heavy-metal stress.

To further characterize the potential roles played by keystone taxa in the resistance of biocrusts to heavy metals, we assessed the effects and evaluated their contribution to community stability using linear regression (Fig. 6c) and RF models (Fig. 6d). A positive correlation was observed between the relative abundance of keystone taxa and their negative: positive cohesion (*P* < 0.05), demonstrating the strong and significant contributions of keystone taxa to promoting network stability. Using RF analysis, keystone taxa were ranked according to their importance to community stability. The key roles of *Chloroflexi* SBR1031, JG30-KF-CM45, and A4b were demonstrated based on a high IncNodePurity (*i.e.,* ASV49 and ASV337 in group IN; ASV49, ASV576, and ASV123 in group C on day 40; and ASV25 in group C on day 100). In group T, on day 40, ASV61 (*Saprospiraceae*) and ASV16 (*Chryseolinea*) played key roles in maintaining community stability, whereas on day 100, ASV438 (*Sandarakinorhabdus*) was the greatest contributor.
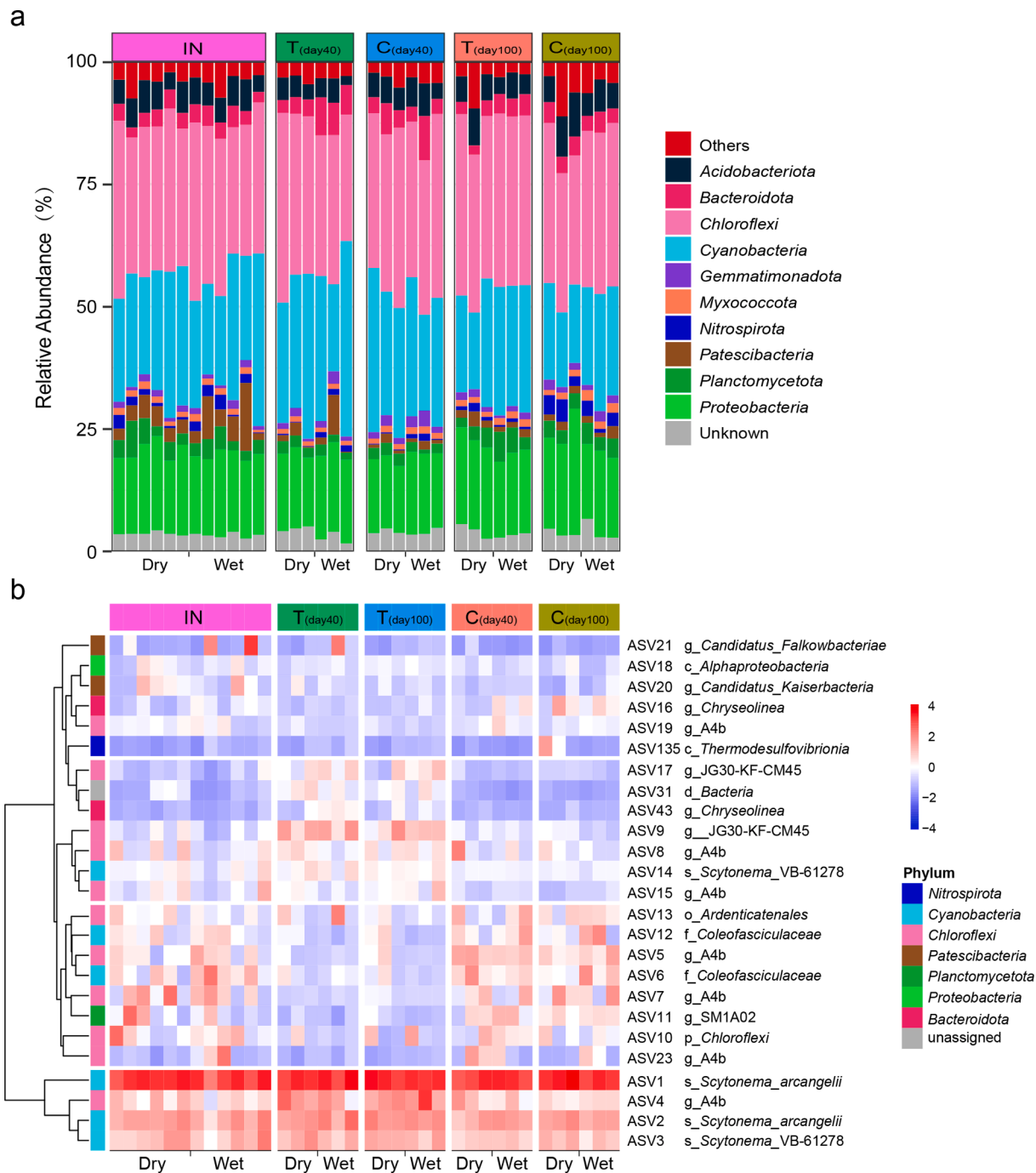
Fig. 4. Detailed microbial community succession of biocrusts during incubation. (a) Stacked bar chart of the phylum-level distribution; phyla with relative abundance below the top 10 are listed as 'Others'. (b) Heatmap of the top 10 ASVs in relative abundance in each group. IN means the initial condition of biocrusts at the beginning of the incubation, T and C represent groups with and without heavy-metal stress, respectively, and D and W represent groups under dry and wet water conditions, respectively.

4. Discussion

4.1. Specific characteristics of biocrusts in tailing wetlands

Biocrusts in humid environments have received minimal research attention (Thomas et al., 2006; Wang et al., 2022a). Differences in climatic conditions may significantly affect biocrust formation and succession, for which microorganisms are the primary driver (Belnap, 2003b; Belnap et al., 2006; Weber et al., 2015), especially for those conditions to which microorganisms were sensitive. Therefore, given that water is the environmental factor that differs the most between arid

and humid regions, inducing active microbial metabolism (Weber et al., 2016) and heavy-metal stress is recognized as an influencer of microbiota structure (Fashola et al., 2016; Wang et al., 2024), these two factors might be essential drivers of biocrust uniqueness in tailing wetlands.

In the current study, biocrusts in tailing wetlands were more hydrophobic and twice as thick as those in previous studies (1–6 mm) (Colesie et al., 2016). Moreover, biocrust water repellency in tailing wetlands was stronger than that previously reported. The WDPT of the desert and induced cyanobacterial biocrusts were 0.5–5 s, much lower than in the tailing wetland (Table 1) (Yang et al., 2014; Keck et al., 2016; Mugnai et al., 2018). Such characteristics might be attributed to less-
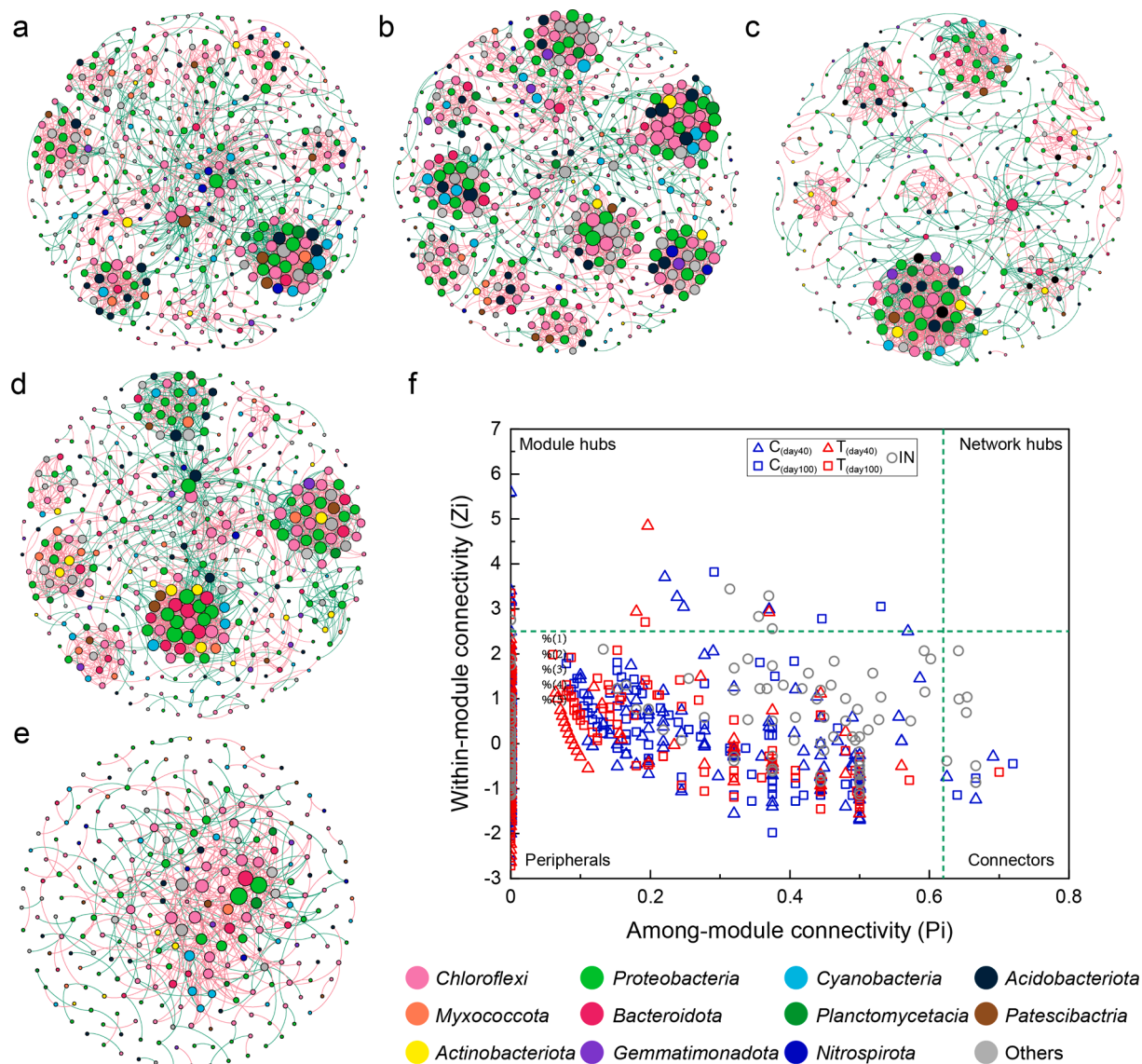
Fig. 5. Microbial co-occurrence networks of ASVs based on 16S rRNA genes and keystone taxa determination. To reveal the influence of heavy metals on microbial community succession dynamics, networks of group C at day 40 (a) and day 100 (b), group T at day 40 (c) and day 100 (d), and group IN (e) were established. The node size is dependent on the node degree, and the colors are based on their phylum (*e.g., Chloroflexi, Proteobacteria*, and *Cyanobacteria*). Green and red links represent positive and negative interactions, respectively. (f) Zi (within-module connectivity)-Pi (among-module connectivity) plot showing the roles of the nodes in microbial co-occurrence networks. IN means the initial condition of biocrusts at the beginning of the incubation, and T and C represent groups with and without heavy-metal stress, respectively.

constrained microbial activity provided by adequate water and the effects of heavy metals on the microbiota composition and metabolism. Without water limitations, mechanical winding of soil particles by filamentous microorganisms, such as *Cyanobacteria* (Fig. 1c, e), and soil particle conglutination by EPS would be enhanced by stronger and more sustained microbial activity (Zhang et al., 2006; Mugnai et al., 2018; Witzgall et al., 2021). Under heavy-metal stress, enrichment of *Cyanobacteria* (Fig. 4a) and greater secretion of EPS further increases the thickness (Venter et al., 2018; Naveed et al., 2019). Moreover, under adequate water conditions, swollen *Cyanobacteria* and EPS clog soil pores, contributing to stronger water repellency and a stable anaerobic environment (Fischer et al., 2010).

Wetland biocrusts also showed increased carbon and nitrogen fixation over desert crusts. The wetland in this study was constructed in 2017; over four years of ecological succession, TC and TN content in the biocrusts increased by 3.3 and 8.7 times (Table 1) compared with those in tailing sand, respectively. Meanwhile, they were consistent with

natural or induced desert biocrusts that developed over a decade in the study by Deng et al. (2020). The carbon and nitrogen contents of biocrusts from nine sites in four deserts investigated by Strauss et al. (2012) were also lower than those in the study area. Such fixation capacity might be due to less-constrained microbial activity caused by adequate water. Therefore, sufficient water and heavy-metal stress shape the distinct characteristics of biocrusts in tailing wetlands.

4.2. Survival strategies for heavy-metal stress

During incubation, the variation in water content exerted a limited impact on the biocrust microbial composition based on the results of RM-ANOVA and PERMANOVA tests (Fig. 3a, Tables S3, S4, S11, S12). Therefore, the changes in microbial community structure and co-occurrence networks observed in the indoor pot incubation can be attributed to the influence of heavy-metal stress. Most heavy metals enriched in group T were in potentially bioavailable fractions (Fig. 2b, c,

Table 2
Topological properties of the empirical networks of the microbial community in different groups and their associated random networks.

Group name	Empirical networks										Random networks		Modularity (M ± SD)
	Network size (n)	Positive Links	Negative Links	Network Indexes	Average degree (avgK)	Average clustering coefficient (avgCC)	Harmonic geodesic distance (HD)	Transitivity (Trans)	Modularity (fast greedy)	Small-world coefficient σ [a]	Average clustering coefficient (avgCC ± SD)	Harmonic geodesic distance (HD ± SD)	
C[b] (day 40)	458	656	989	0.94	7.183	0.261	4.738	0.327	0.787	4.899	0.034 ± 0.005	3.024 ± 0.013	0.330 ± 0.005
C (day 100)	492	556	1446	0.95	8.138	0.28	5.011	0.327	0.831	5.543	0.030 ± 0.004	2.976 ± 0.013	0.304 ± 0.005
T[c] (day 40)	358	522	779	0.95	7.531	0.271	4.516	0.325	0.738	2.969	0.058 ± 0.006	2.870 ± 0.018	0.306 ± 0.004
T (day 100)	417	732	1027	0.95	8.436	0.285	4.564	0.332	0.772	3.950	0.045 ± 0.004	2.850 ± 0.015	0.291 ± 0.004
IN[d]	267	175	356	0.84	3.978	0.077	3.737	0.099	0.579	1.748	0.039 ± 0.007	3.309 ± 0.043	0.477 ± 0.006

[a] Small-world coefficient $\sigma = (CC/CC_r)/(HD/HD_r)$, where subscript r indicates the properties of the random networks
[b] C represents groups without heavy-metal stress.
[c] T represents groups with heavy-metal stress.
[d] IN represents the initial condition of biocrusts at the beginning of the incubation.

Fig. S6), which were more toxic and easier to accumulate (Kim et al., 2015). Microbial metabolism and turnover, including organic compound biodegradation and carbon production, can also be inhibited by bioavailable heavy metals (Dell'Anno et al., 2003; Olaniran et al., 2013; Gui et al., 2017; Xu et al., 2021). However, microbial-mediated carbon and nitrogen fixation was not significantly inhibited by heavy metals in this study (Tables S9, S10). During photosynthetic carbon fixation, algae tend to accumulate inorganic carbonates, increasing the environmental pH (Bwapwa et al., 2017); meanwhile, heavy-metal stress did not significantly impact the biocrust pH during incubation. (Table S5). Biocrusts in tailing wetlands likely have unique survival strategies to adapt to heavy metals.

4.2.1. Higher level of succession for stronger resistance driven by Cyanobacteria

Our evaluation of succession showed that community resistance gradually increased with the complexity of the redundant structure. The dominant photosynthetic microorganism is an indicator of biocrust succession (Muñoz-Martín et al., 2019). In our study, the relative abundance of *Coleofasciculaceae* decreased by 63 % under heavy-metal stress (Fig. S9b). Thus, crusts for which the predominant photoautotrophs are *Coleofasciculaceae* are designated "light cyanobacterial crusts," representing an early stage of cyanobacterial crust (Muñoz-Martín et al., 2019; Fernandes et al., 2021). In contrast, the relative abundance of *Scytonema* increased by 59 % under heavy-metal stress (Fig. S9a). *Scytonema*, a nonmotile heterocystous *Cyanobacteria*, characterizes biocrusts in which it is the dominant photoautotroph as "dark cyanobacterial crusts," signifying a higher degree of succession (Dojani et al., 2011; Muñoz-Martín et al., 2019). Therefore, biocrusts appeared to prefer a higher level of succession under heavy-metal stress, which would enhance their resistance to environmental stresses (Colin et al., 2019). Moreover, *Scytonema* is also capable of alkali production and nitrogen fixation (Komárek, 2003; Muñoz-Martín et al., 2019). A higher pH would reduce the mobility of heavy metals and increased nitrogen would relieve the nitrogen limitation on microorganism growth (Bwapwa et al., 2017; Sun et al., 2020a). Therefore, such a succession strategy likely helps biocrusts adapt to and immobilize heavy metals. This might account for the relatively constant carbon and nitrogen levels under heavy-metal stress (Fig. 2e, f).

4.2.2. Active nitrogen-cycling trait for nitrogen turnover maintained by the high abundance and connectivity of related microorganisms

Harsh ecosystems often recruit nitrogen-fixing microbes to provide essential nutrients to their successors (Mendez et al., 2008). Although chemolithoautotrophic bacteria are considered to dominate the nitrogen fixation process in mining regions due to the high concentration of sulfur and metal compounds (Sun et al., 2020a), *Cyanobacteria* were abundant in the biocrust-covered mining regions (Nyenda et al., 2019; Xiao et al., 2022). Nitrogen supplementation can facilitate growth and adaptation to the challenging mining environment (Fierer et al., 2012). Therefore, as photosynthetic nitrogen-fixing microorganisms, *Cyanobacteria* exhibit high connectivity and represent major hubs in co-occurrence networks (Pombubpa et al., 2020; Wang et al., 2022a). Although *Cyanobacteria* was also the predominant phylum in this study, only one *Cyanobacteria* ASV was regarded as a keystone taxon (Table S1). In contrast, microbes with the potential to participate in the denitrification process, such as *Chloroflexi* JG30-KF-CM45, A4b, and SBR1031 (Li et al., 2021; Nguyen Quoc et al., 2021; Shi et al., 2022), maintained high relative abundance (Fig. 4b). Moreover, 48 % of the keystone taxa had the potential to participate in the inorganic nitrogen cycle and played the most important role in network stability, excluding in group T on day 100 (Fig. 6d). These microbes, commonly found in sludge and compost, are recruited to biocrusts (Li et al., 2021; Nguyen Quoc et al., 2021; Shi et al., 2022; Wang et al., 2022b), potentially due to the anaerobic environment created by the swollen EPS and Cyanobacteria clogging the soil pores and the sufficient water in the wetland (Fischer et al., 2010). These
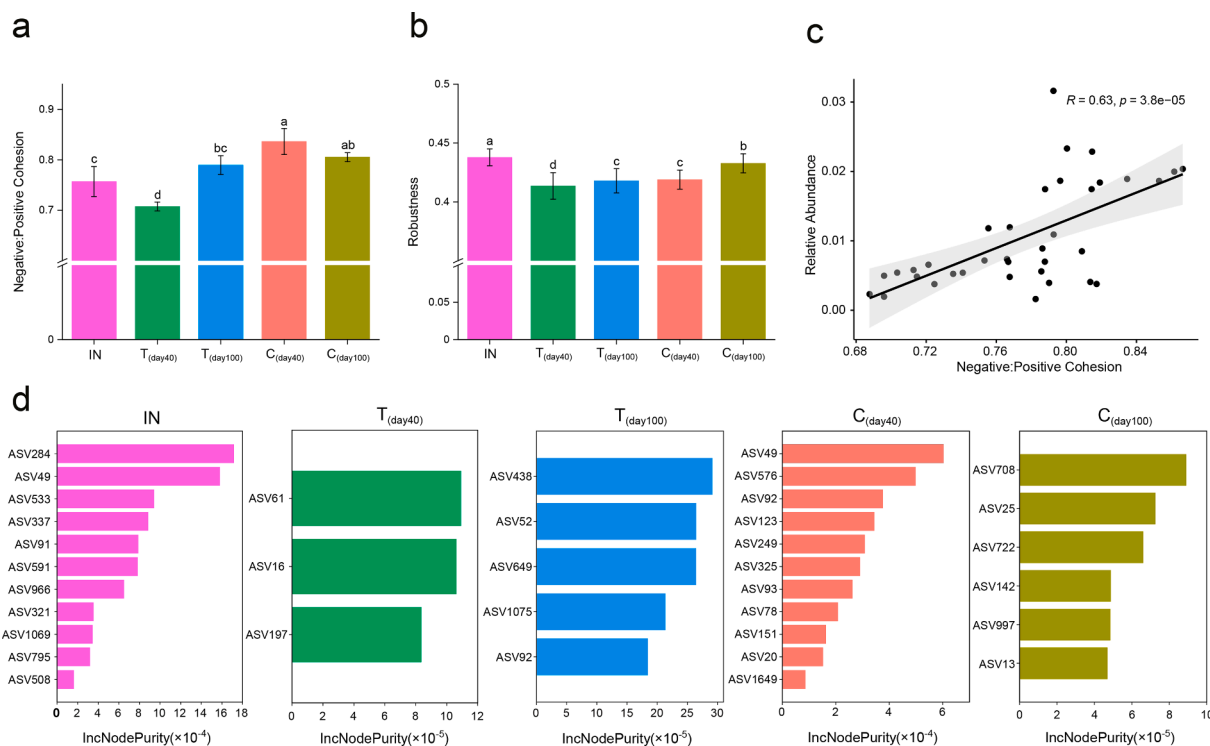
Fig. 6. Community stability in different groups and contribution of keystone taxa. (a) Robustness. (b) Negative: positive cohesion. (c) Linear regression analysis between the relative abundance of keystone taxa and the negative: positive cohesion. The black line represents the linear trendline, and the shaded area represents the 95 % confidence interval. (d) RF analysis predicting the contribution of keystone ASVs to community stability. IN means the initial condition of biocrusts at the beginning of the incubation, and T and C represent groups with and without heavy-metal stress, respectively.

microbes could contribute to the active inorganic nitrogen cycling, leading to stronger nitrogen turnover, as a strong correlation has been reported between the frequencies of each process in the nitrogen cycle (Nelson et al., 2016). Such efficient nitrogen turnover would ensure better utilization of scarce nitrogen (Kuypers et al., 2018), which may represent a second biocrust survival strategy under heavy-metal stress.

Notably, in group T on day 100, 40 % of the keystone taxa were closely related to EPS secretion and biofilm formation (Table S1), particularly ASV438 (*Sandarakinorhabdus*), which was the most important taxon for maintaining the microbial network stability (Fig. 6d) and represents the core microbiome of biofilms (Di Gregorio et al., 2017; de Sousa Rollemberg et al., 2018). Considering that increased EPS secretion under heavy-metal stress is a key mechanism by which microorganisms resist toxicity (Naveed et al., 2019), the inorganic nitrogen cycle-related microbes in biocrusts might struggle to maintain high connectivity under long-term heavy-metal stress and recruit microbes with key roles in EPS secretion and initial biofilm formation as a defense mechanism. The succession of keystone taxa suggests that the co-occurrence patterns of biocrusts may not function optimally under long-term heavy-metal stress.

4.2.3. Close-knit community for high microbial connectivity created by greater cooperation

Maintaining efficient inorganic nitrogen turnover requires close cooperation among microorganisms, therefore, the topological properties of microbial co-occurrence networks also reveal the survival strategy of biocrusts. Fewer nodes and edges with a higher avgCC in the co-occurrence networks (Table 2) under heavy-metal stress indicated that although microbial interactions were inhibited, fewer nodes maintained connectivity by changing co-occurrence patterns to form a relatively close-knit community (Barberán et al., 2012; Yuan et al., 2021b). This can be reflected in microbial interactions as the proportion of positive linkages in the networks (Table 2) and positive cohesion (Fig. S10) were

increased under heavy-metal stress. Both factors could induce more positive relationships, reflecting greater cooperation (Hernandez et al., 2021; She et al., 2021). As a typical type of cooperation, exchanging compounds such as vitamin B_{12} and organic carbon could establish mutualistic partnerships between heterotrophs and autotrophs, helping them adapt to extreme environments (Oliveira et al., 2014; Krug et al., 2020; You et al., 2021). Increased cooperation can also increase the overall metabolic efficiency of communities. (Coyte et al., 2015). Therefore, a close-knit community may promote microbial metabolism and substance turnover, potentially representing a third survival strategy.

However, a higher ratio of positive interactions also indicates weaker networks as cooperation can induce negative feedback when one member in the positive network decreases in abundance (Hernandez et al., 2021). Perturbations could also be rapidly propagated throughout the network, decreasing network efficiency (Oliveira et al., 2014; Yuan et al., 2021a), potentially accounting for the lower small-world coefficient σ in group C (Table 2). Therefore, this strategy may not function well under long-term heavy-metal stress, which is supported by the keystone taxa succession.

5. Conclusion

In summary, biocrusts in tailing wetlands exhibit thicker and more hydrophobic structures, along with more active microbial activity, resulting from less-constrained metabolism due to adequate water and the influence of heavy metals. Three key potential survival strategies that enable biocrusts to thrive under heavy-metal stress have been identified: (1) succession to a higher level of cyanobacterial crusts; (2) maintaining high abundance and connectivity of inorganic nitrogen cycle-related microorganisms; and (3) creating a closer-knit community through greater cooperation. Further analyses of microbial-driven heavy-metal resistance and immobilization mechanisms of biocrusts

based on identifying related functional genes or metagenomic analysis could provide more in-depth insights into these heavy-metal survival strategies.

Data accessibility

The raw sequence data described in this paper have been deposited in the Genome Sequence Archive (Chen et al., 2021) in the National Genomics Data Center (CNCB-NGDC Members Partners, 2022), China National Center for Bioinformatics/Beijing Institute of Genomics, Chinese Academy of Sciences, under accession number CRA009811. They are publicly accessible at https://ngdc.cncb.ac.cn/gsa.

CRediT authorship contribution statement

Zekai Feng: Conceptualization, Data curation, Formal analysis, Investigation, Methodology, Validation, Visualization, Writing – original draft, Writing – review & editing. **Guobao Wang:** Conceptualization, Funding acquisition, Investigation, Supervision, Writing – review & editing. **Yuanyuan Jiang:** Investigation, Methodology. **Chiyu Chen:** Investigation, Formal analysis. **Daijie Chen:** Investigation, Methodology. **Mengyao Li:** Investigation, Methodology. **Jean Louis Morel:** Validation, Supervision, Writing – review & editing. **Hang Yu:** Investigation. **Yuanqing Chao:** Methodology, Supervision, Validation, Writing – review & editing. **Yetao Tang:** Supervision, Validation, Writing – review & editing. **Rongliang Qiu:** Supervision, Validation, Writing – review & editing. **Shizhong Wang:** Conceptualization, Funding acquisition, Project administration, Supervision, Validation, Writing – review & editing, Methodology.

Declaration of competing interest

The authors declare that they have no known competing financial interests or personal relationships that could have appeared to influence the work reported in this paper.

Appendix A. Supplementary data

Supplementary data to this article can be found online at https://doi.org/10.1016/j.geoderma.2024.116852.

References

Barberán, A., Bates, S.T., Casamayor, E.O., Fierer, N., 2012. Using network analysis to explore co-occurrence patterns in soil microbial communities. ISME J. 6 (2), 343–351. https://doi.org/10.1038/ismej.2011.119.

Bardgett, R.D., van der Putten, W.H., 2014. Belowground biodiversity and ecosystem functioning. Nature 515 (7528), 505–511. https://doi.org/10.1038/nature13855.

Bardou, P., Mariette, J., Escudié, F., Djemiel, C., Klopp, C., 2014. jvenn: an interactive venn diagram viewer. BMC Bioinf. 15 (1), 293. https://doi.org/10.1186/1471-2105-15-293.

Bastian, M., Heymann, S., Jacomy, M., 2009. Gephi: an open source software for exploring and manipulating networks. Proceedings of the International AAAI Conference on Web and Social Media 3 (1), 361–362. https://doi.org/10.1609/icwsm.v3i1.13937.

Belnap, J., 2003a. Microbes and microfauna associated with biological soil crusts. In: Belnap, J., Lange, O.L. (Eds.), Biological Soil Crusts: Structure, Function, and Management. Springer Berlin Heidelberg, Berlin, Heidelberg, pp. 167–174. https://doi.org/10.1007/978-3-642-56475-8_14.

Belnap, J., 2003b. The world at your feet: desert biological soil crusts. Front. Ecol. Environ. 1 (4), 181–189. https://doi.org/10.1890/1540-9295(2003)001[0181:TWAYFD]2.0.CO;2.

Belnap, J., Phillips, S.L., Troxler, T., 2006. Soil lichen and moss cover and species richness can be highly dynamic: the effects of invasion by the annual exotic grass *Bromus tectorum*, precipitation, and temperature on biological soil crusts in SE Utah. Appl. Soil. Ecol. 32 (1), 63–76. https://doi.org/10.1016/j.apsoil.2004.12.010.

Bolyen, E., Rideout, J.R., Dillon, M.R., Bokulich, N.A., Abnet, C.C., Al-Ghalith, G.A., Alexander, H., Alm, E.J., Arumugam, M., Asnicar, F., Bai, Y., Bisanz, J.E., Bittinger, K., Brejnrod, A., Brislawn, C.J., Brown, C.T., Callahan, B.J., Caraballo-Rodríguez, A.M., Chase, J., Cope, E.K., Da Silva, R., Diener, C., Dorrestein, P.C., Douglas, G.M., Durall, D.M., Duvallet, C., Edwardson, C.F., Ernst, M., Estaki, M., Fouquier, J., Gauglitz, J.M., Gibbons, S.M., Gibson, D.L., Gonzalez, A., Gorlick, K., Guo, J., Hillmann, B., Holmes, S., Holste, H., Huttenhower, C., Huttley, G.A., Janssen, S., Jarmusch, A.K., Jiang, L., Kaehler, B.D., Kang, K.B., Keefe, C.R., Keim, P., Kelley, S.T., Knights, D., Koester, I., Kosciolek, T., Kreps, J., Langille, M.G.I., Lee, J., Ley, R., Liu, Y.-X., Loftfield, E., Lozupone, C., Maher, M., Marotz, C., Martin, B.D., McDonald, D., McIver, L.J., Melnik, A.V., Metcalf, J.L., Morgan, S.C., Morton, J.T., Naimey, A.T., Navas-Molina, J.A., Nothias, L.F., Orchanian, S.B., Pearson, T., Peoples, S.L., Petras, D., Preuss, M.L., Pruesse, E., Rasmussen, L.B., Rivers, A., Robeson, M.S., Rosenthal, P., Segata, N., Shaffer, M., Shiffer, A., Sinha, R., Song, S.J., Spear, J.R., Swafford, A.D., Thompson, L.R., Torres, P.J., Trinh, P., Tripathi, A., Turnbaugh, P.J., Ul-Hasan, S., van der Hooft, J.J.J., Vargas, F., Vázquez-Baeza, Y., Vogtmann, E., von Hippel, M., Walters, W., Wan, Y., Wang, M., Warren, J., Weber, K.C., Williamson, C.H.D., Willis, A.D., Xu, Z.Z., Zaneveld, J.R., Zhang, Y., Zhu, Q., Knight, R., Caporaso, J.G., 2019. Reproducible, interactive, scalable and extensible microbiome data science using QIIME 2. Nat. Biotechnol. 37 (8), 852–857. https://doi.org/10.1038/s41587-019-0209-9.

Brady, J.P., Kinaev, I., Goonetilleke, A., Ayoko, G.A., 2016. Comparison of partial extraction reagents for assessing potential bioavailability of heavy metals in sediments. Mar. Pollut. Bull. 106 (1), 329–334. https://doi.org/10.1016/j.marpolbul.2016.03.029.

Bwapwa, J.K., Jaiyeola, A.T., Chetty, R., 2017. Bioremediation of acid mine drainage using algae strains: a review. S. Afr. J. Chem. Eng. 24, 62–70. https://doi.org/10.1016/j.sajce.2017.06.005.

Caesar, J., Tamm, A., Ruckteschler, N., Leifke, A.L., Weber, B., 2018. Revisiting chlorophyll extraction methods in biological soil crusts – methodology for determination of chlorophyll a and chlorophyll a + b as compared to previous methods. Biogeosciences 15 (5), 1415–1424. https://doi.org/10.5194/bg-15-1415-2018.

Calderón, K., Spor, A., Breuil, M.-C., Bru, D., Bizouard, F., Violle, C., Barnard, R.L., Philippot, L., 2017. Effectiveness of ecological rescue for altered soil microbial communities and functions. ISME J. 11 (1), 272–283. https://doi.org/10.1038/ismej.2016.86.

Chen, T., Chen, X., Zhang, S., Zhu, J., Tang, B., Wang, A., Dong, L., Zhang, Z., Yu, C., Sun, Y., Chi, L., Chen, H., Zhai, S., Sun, Y., Lan, L., Zhang, X., Xiao, J., Bao, Y., Wang, Y., Zhang, Z., Zhao, W., 2021. The genome sequence archive family: toward explosive data growth and diverse data types. Genomics, Proteomics Bioinf. 19 (4), 578–583. https://doi.org/10.1016/j.gpb.2021.08.001.

Chun, S.-J., Kim, Y.-J., Cui, Y., Nam, K.-H., 2021. Ecological network analysis reveals distinctive microbial modules associated with heavy metal contamination of abandoned mine soils in Korea. Environ. Pollut. 289, 117851 https://doi.org/10.1016/j.envpol.2021.117851.

Chung, A.P., Coimbra, C., Farias, P., Francisco, R., Branco, R., Simão, F.V., Gomes, E., Pereira, A., Vila, M.C., Fiúza, A., Mortensen, M.S., Sørensen, S.J., Morais, P.V., 2019. Tailings microbial community profile and prediction of its functionality in basins of tungsten mine. Sci. Rep. 9 (1), 19596. https://doi.org/10.1038/s41598-019-55706-6.

Ciccazzo, S., Esposito, A., Borruso, L., Brusetti, L., 2016. Microbial communities and primary succession in high altitude mountain environments. Ann. Microbiol. 66 (1), 43–60. https://doi.org/10.1007/s13213-015-1130-1.

CNCB-NGDC Members Partners, 2022. Database resources of the National Genomics Data Center, China National Center for bioinformation in 2022. Nucleic Acids Res. 50 (D1), D27–D38. https://doi.org/10.1093/nar/gkab951.

Colesie, C., Felde, V.J.M.N.L., Büdel, B., 2016. Composition and macrostructure of biological soil crusts. In: Weber, B., Büdel, B., Belnap, J. (Eds.), Biological Soil Crusts: an Organizing Principle in Drylands. Springer International Publishing, Cham, pp. 159–172. https://doi.org/10.1007/978-3-319-30214-0_9.

Colin, Y., Goberna, M., Verdú, M., Navarro-Cano, J.A., 2019. Successional trajectories of soil bacterial communities in mine tailings: the role of plant functional traits. J. Environ. Manage. 241, 284–292. https://doi.org/10.1016/j.jenvman.2019.04.023.

Coyte, K.Z., Schluter, J., Foster, K.R., 2015. The ecology of the microbiome: networks, competition, and stability. Science 350 (6261), 663–666. https://doi.org/10.1126/science.aad2602.

Cutler, D.R., Edwards Jr, T.C., Beard, K.H., Cutler, A., Hess, K.T., Gibson, J., Lawler, J.J., 2007. Random forests for classification in ecology. Ecology 88 (11), 2783–2792. https://doi.org/10.1890/07-0539.1.

Cydzik-Kwiatkowska, A., 2015. Bacterial structure of aerobic granules is determined by aeration mode and nitrogen load in the reactor cycle. Bioresour. Technol. 181, 312–320. https://doi.org/10.1016/j.biortech.2015.01.101.

de Sousa Rollemberg, S.L., Mendes Barros, A.R., Milen Firmino, P.I., Bezerra Dos Santos, A., 2018. Aerobic granular sludge: cultivation parameters and removal mechanisms. Bioresour. Technol. 270, 678–688. https://doi.org/10.1016/j.biortech.2018.08.130.

Dell'Anno, A., Mei, M.L., Ianni, C., Danovaro, R., 2003. Impact of bioavailable heavy metals on bacterial activities in coastal marine sediments. World J. Microbiol. Biotechnol. 19 (1), 93–100. https://doi.org/10.1023/A:1022581632116.

Deng, S., Zhang, D., Wang, G., Zhou, X., Ye, C., Fu, T., Ke, T., Zhang, Y., Liu, Y., Chen, L., 2020. Biological soil crust succession in deserts through a 59-year-long case study in China: how induced biological soil crust strategy accelerates desertification reversal from decades to years. Soil Biol. Biochem. 141, 107665 https://doi.org/10.1016/j.soilbio.2019.107665.

Di Gregorio, L., Tandoi, V., Congestri, R., Rossetti, S., Di Pippo, F., 2017. Unravelling the core microbiome of biofilms in cooling tower systems. Biofouling 33 (10), 793–806. https://doi.org/10.1080/08927014.2017.1367386.

Dojani, S., Büdel, B., Deutschewitz, K., Weber, B., 2011. Rapid succession of biological soil crusts after experimental disturbance in the succulent Karoo. South Africa. Appl. Soil. Ecol. 48 (3), 263–269. https://doi.org/10.1016/j.apsoil.2011.04.013.

Falkowski, P.G., Fenchel, T., Delong, E.F., 2008. The microbial engines that drive earth's biogeochemical cycles. Science 320 (5879), 1034–1039. https://doi.org/10.1126/science.1153213.

Fashola, M.O., Ngole-Jeme, V.M., Babalola, O.O., 2016. Heavy metal pollution from gold mines: environmental effects and bacterial strategies for resistance. Int. J. Environ. Res. Public Health 13 (11), 1047. https://doi.org/10.3390/ijerph13111047.

Fernandes, V.M.C., Giraldo-Silva, A., Roush, D., Garcia-Pichel, F., 2021. *Coleofasciculaceae*, a monophyletic home for the *Microcoleus steenstrupii* complex and other desiccation-tolerant filamentous cyanobacteria. J. Phycol. 57 (5), 1563–1579. https://doi.org/10.1111/jpy.13199.

Fierer, N., Lauber, C.L., Ramirez, K.S., Zaneveld, J., Bradford, M.A., Knight, R., 2012. Comparative metagenomic, phylogenetic and physiological analyses of soil microbial communities across nitrogen gradients. ISME J. 6 (5), 1007–1017. https://doi.org/10.1038/ismej.2011.159.

Fischer, T., Veste, M., Wiehe, W., Lange, P., 2010. Water repellency and pore clogging at early successional stages of microbiotic crusts on inland dunes, Brandenburg. NE Germany. Catena 80 (1), 47–52. https://doi.org/10.1016/j.catena.2009.08.009.

Gauthier, P.T., Norwood, W.P., Prepas, E.E., Pyle, G.G., 2014. METAL–PAH mixtures in the aquatic environment: a review of co-toxic mechanisms leading to more-than-additive outcomes. Aquat. Toxicol. 154, 253–269. https://doi.org/10.1016/j.aquatox.2014.05.026.

Gui, M., Chen, Q., Ma, T., Zheng, M., Ni, J., 2017. Effects of heavy metals on aerobic denitrification by strain *pseudomonas stutzeri* PCN-1. Appl. Microbiol. Biotechnol. 101 (4), 1717–1727. https://doi.org/10.1007/s00253-016-7984-8.

Guo, M., Zhong, X., Liu, W., Wang, G., Chao, Y., Huot, H., Qiu, R., Morel, J.L., Watteau, F., Séré, G., Tang, Y., 2022. Biogeochemical dynamics of nutrients and rare earth elements (REEs) during natural succession from biocrusts to pioneer plants in REE mine tailings in southern China. Sci. Total. Environ. 828, 154361 https://doi.org/10.1016/j.scitotenv.2022.154361.

Hernandez, D.J., David, A.S., Menges, E.S., Searcy, C.A., Afkhami, M.E., 2021. Environmental stress destabilizes microbial networks. ISME J. 15 (6), 1722–1734. https://doi.org/10.1038/s41396-020-00882-x.

Herren, C.M., McMahon, K.D., 2017. Cohesion: a method for quantifying the connectivity of microbial communities. ISME J. 11 (11), 2426–2438. https://doi.org/10.1038/ismej.2017.91.

Huang, X., Du, H., Deng, X., Chen, Y., Xiang, L., Li, Y., Li, H., Mo, C., Cai, Q., Zhao, H., 2021. New insights into the evolution of bacterial community during the domestication of phthalate-degrading consortium. J. Clean. Prod. 303, 127064 https://doi.org/10.1016/j.jclepro.2021.127064.

Huang, L., Tang, F., Song, Y., Wan, C., Wang, S., Liu, W., Shu, W., 2011. Biodiversity, abundance, and activity of nitrogen-fixing bacteria during primary succession on a copper mine tailings. FEMS Microbiol. Ecol. 78 (3), 439–450. https://doi.org/10.1111/j.1574-6941.2011.01178.x.

Jiao, S., Chen, W., Wang, J., Du, N., Li, Q., Wei, G., 2018. Soil microbiomes with distinct assemblies through vertical soil profiles drive the cycling of multiple nutrients in reforested ecosystems. Microbiome 6 (1), 146. https://doi.org/10.1186/s40168-018-0526-0.

Keck, H., Felde, V.J.M.N.L., Drahorad, S.L., Felix-Henningsen, P., 2016. Biological soil crusts cause subcritical water repellency in a sand dune ecosystem located along a rainfall gradient in the NW Negev desert. Israel. J. Hydrol. Hydromech. 64 (2), 133–140. https://doi.org/10.1515/johh-2016-0001.

Kim, R.-Y., Yoon, J.-K., Kim, T.-S., Yang, J.E., Owens, G., Kim, K.-R., 2015. Bioavailability of heavy metals in soils: definitions and practical implementation—a critical review. Environ. Geochem. Health. 37 (6), 1041–1061. https://doi.org/10.1007/s10653-015-9695-y.

Komárek, J., 2003. Coccoid and colonial *cyanobacteria*. In: Wehr, J.D., Sheath, R.G. (Eds.), Freshwater Algae of North America. Academic Press, Burlington, pp. 59–116. https://doi.org/10.1016/B978-012741550-5/50004-0.

Kratz, A.M., Maier, S., Weber, J., Kim, M., Mele, G., Gargiulo, L., Leifke, A.L., Prass, M., Abed, R.M.M., Cheng, Y., Su, H., Pöschl, U., Weber, B., 2022. Reactive nitrogen hotspots related to microscale heterogeneity in biological soil crusts. Environ. Sci. Technol. 56 (16), 11865–11877. https://doi.org/10.1021/acs.est.2c02207.

Krug, L., Erlacher, A., Markut, K., Berg, G., Cernava, T., 2020. The microbiome of alpine snow algae shows a specific inter-kingdom connectivity and algae-bacteria interactions with supportive capacities. ISME J. 14 (9), 2197–2210. https://doi.org/10.1038/s41396-020-0677-4.

Kuypers, M.M.M., Marchant, H.K., Kartal, B., 2018. The microbial nitrogen-cycling network. Nat. Rev. Microbiol. 16 (5), 263–276. https://doi.org/10.1038/nrmicro.2018.9.

Li, H., Wang, X., Wu, Y., Zhang, D., Xu, H., Xu, H., Xing, X., Qi, Z., 2021. Relationships among bedding materials, bedding bacterial composition and lameness in dairy cows. Anim. Biosci. 34 (9), 1559–1568. https://doi.org/10.5713/ajas.20.0565.

Liang, Y., Yi, X., Dang, Z., Wang, Q., Luo, H., Tang, J., 2017. Heavy metal contamination and health risk assessment in the vicinity of a tailing pond in Guangdong, China. Int. J. Environ. Res. Public Health 14 (12). https://doi.org/10.3390/ijerph14121557.

Liu, W., Song, Y., Wang, B., Li, J., Shu, W., 2012. Nitrogen fixation in biotic crusts and vascular plant communities on a copper mine tailings. Eur. J. Soil Biol. 50, 15–20. https://doi.org/10.1016/j.ejsobi.2011.11.009.

Liu, S., Yu, H., Yu, Y., Huang, J., Zhou, Z., Zeng, J., Chen, P., Xiao, F., He, Z., Yan, Q., 2022. Ecological stability of microbial communities in Lake donghu regulated by keystone taxa. Ecol. Indic. 136, 108695 https://doi.org/10.1016/j.ecolind.2022.108695.

Maier, S., Kratz, A.M., Weber, J., Prass, M., Liu, F., Clark, A.T., Abed, R.M.M., Su, H., Cheng, Y., Eickhorst, T., Fiedler, S., Pöschl, U., Weber, B., 2021. Water-driven microbial nitrogen transformations in biological soil crusts causing atmospheric nitrous acid and nitric oxide emissions. ISME J. 16, 1012–1024. https://doi.org/10.1038/s41396-021-01127-1.

Mendez, M.O., Neilson, J.W., Maier, R.M., 2008. Characterization of a bacterial community in an abandoned semiarid lead-zinc mine tailing site. Appl. Environ. Microbiol. 74 (12), 3899–3907. https://doi.org/10.1128/AEM.02883-07.

Mingorance, M.D., Barahona, E., Fernández-Gálvez, J., 2007. Guidelines for improving organic carbon recovery by the wet oxidation method. Chemosphere 68 (3), 409–413. https://doi.org/10.1016/j.chemosphere.2007.01.021.

Miya, M., Sato, Y., Fukunaga, T., Sado, T., Poulsen, J.Y., Sato, K., Minamoto, T., Yamamoto, S., Yamanaka, H., Araki, H., Kondoh, M., Iwasaki, W., 2015. MiFish, a set of universal PCR primers for metabarcoding environmental DNA from fishes: detection of more than 230 subtropical marine species. R. Soc. Open Sci. 2 (7), 150088 https://doi.org/10.1098/rsos.150088.

Mugnai, G., Rossi, F., Felde, V.J.M.N.L., Colesie, C., Büdel, B., Peth, S., Kaplan, A., De Philippis, R., 2018. The potential of the cyanobacterium *leptolyngbya ohadii* as inoculum for stabilizing bare sandy substrates. Soil Biol. Biochem. 127, 318–328. https://doi.org/10.1016/j.soilbio.2018.08.007.

Muñoz-Martín, M.Á., Becerra-Absalón, I., Perona, E., Fernández-Valbuena, L., Garcia-Pichel, F., Mateo, P., 2019. Cyanobacterial biocrust diversity in Mediterranean ecosystems along a latitudinal and climatic gradient. New Phytol. 221 (1), 123–141. https://doi.org/10.1111/nph.15355.

Naveed, S., Li, C., Lu, X., Chen, S., Yin, B., Zhang, C., Ge, Y., 2019. Microalgal extracellular polymeric substances and their interactions with metal(loid)s: a review. Critical Reviews in Environ. Sci. Technol. 49 (19), 1769–1802. https://doi.org/10.1080/10643389.2019.1583052.

Nelson, M.B., Martiny, A.C., Martiny, J.B.H., 2016. Global biogeography of microbial nitrogen-cycling traits in soil. Proc. Natl. Acad. Sci. USA 113 (29), 8033. https://doi.org/10.1073/pnas.1601070113.

Nguyen Quoc, B., Armenta, M., Carter, J.A., Bucher, R., Sukapanpotharam, P., Bryson, S.J., Stahl, D.A., Stensel, H.D., Winkler, M.H., 2021. An investigation into the optimal granular sludge size for simultaneous nitrogen and phosphate removal. Water Res. 198, 117119 https://doi.org/10.1016/j.watres.2021.117119.

Nyenda, T., Gwenzi, W., Piyo, T.T., Jacobs, S.M., 2019. Occurrence of biological crusts and their relationship with vegetation on a chronosequence of abandoned gold mine tailings. Ecol. Eng. 139, 105559 https://doi.org/10.1016/j.ecoleng.2019.07.029.

Olaniran, A.O., Balgobind, A., Pillay, B., 2013. Bioavailability of heavy metals in soil: impact on microbial biodegradation of organic compounds and possible improvement strategies. Int. J. Mol. Sci. 14 (5), 10197–10228. https://doi.org/10.3390/ijms140510197.

Oliveira, N.M., Niehus, R., Foster, K.R., 2014. Evolutionary limits to cooperation in microbial communities. Proc. Natl. Acad. Sci. USA 111 (50), 17941–17946. https://doi.org/10.1073/pnas.1412673111.

Pombubpa, N., Pietrasiak, N., De Ley, P., Stajich, J.E., 2020. Insights into dryland biocrust microbiome: geography, soil depth and crust type affect biocrust microbial communities and networks in Mojave Desert, USA. FEMS Microbiol. Ecol. 96 (9), fiaa125. https://doi.org/10.1093/femsec/fiaa125.

Qiu, L., Zhang, Q., Zhu, H., Reich, P.B., Banerjee, S., van der Heijden, M.G.A., Sadowsky, M.J., Ishii, S., Jia, X., Shao, M., Liu, B., Jiao, H., Li, H., Wei, X., 2021. Erosion reduces soil microbial diversity, network complexity and multifunctionality. ISME J. 15 (8), 2474–2489. https://doi.org/10.1038/s41396-021-00913-1.

Quast, C., Pruesse, E., Yilmaz, P., Gerken, J., Schweer, T., Yarza, P., Peplies, J., Glöckner, F.O., 2012. The SILVA ribosomal RNA gene database project: improved data processing and web-based tools. Nucleic Acids Res. 41 (D1), D590–D596. https://doi.org/10.1093/nar/gks1219.

Rodriguez-Caballero, E., Belnap, J., Büdel, B., Crutzen, P.J., Andreae, M.O., Pöschl, U., Weber, B., 2018. Dryland photoautotrophic soil surface communities endangered byglobal change. Nat. Geosci. 11 (3), 185–189. https://doi.org/10.1038/s41561-018-0072-1.

She, Z., Pan, X., Wang, J., Shao, R., Wang, G., Wang, S., Yue, Z., 2021. Vertical environmental gradient drives prokaryotic microbial community assembly and species coexistence in a stratified acid mine drainage lake. Water Res. 206, 117739 https://doi.org/10.1016/j.watres.2021.117739.

Shi, S., Lin, Z., Zhou, J., Fan, X., Huang, Y., Zhou, J., 2022. Enhanced thermophilic denitrification performance and potential microbial mechanism in denitrifying granular sludge system. Bioresour. Technol. 344, 126190 https://doi.org/10.1016/j.biortech.2021.126190.

Strauss, S.L., Day, T.A., Garcia-Pichel, F., 2012. Nitrogen cycling in desert biological soil crusts across biogeographic regions in the southwestern United States. Biogeochemistry 108 (1), 171–182. https://doi.org/10.1007/s10533-011-9587-x.

Sun, X., Kong, T., Häggblom, M.M., Kolton, M., Li, F., Dong, Y., Huang, Y., Li, B., Sun, W., 2020a. Chemolithoautotropic diazotrophy dominates the nitrogen fixation process in mine tailings. Environ. Sci. Technol. 54 (10), 6082–6093. https://doi.org/10.1021/acs.est.9b07835.

Sun, W., Xiao, E., Häggblom, M., Krumins, V., Dong, Y., Sun, X., Li, F., Wang, Q., Li, B., Yan, B., 2018. Bacterial survival strategies in an alkaline tailing site and the physiological mechanisms of dominant phylotypes as revealed by metagenomic analyses. Environ. Sci. Technol. 52 (22), 13370–13380. https://doi.org/10.1021/acs.est.8b03853.

Sun, X., Xu, R., Dong, Y., Li, F., Tao, W., Kong, T., Zhang, M., Qiu, L., Wang, X., Sun, W., 2020b. Investigation of the ecological roles of putative keystone taxa during tailing revegetation. Environ. Sci. Technol. 54 (18), 11258–11270. https://doi.org/10.1021/acs.est.0c03031.

Swenson, T.L., Karaoz, U., Swenson, J.M., Bowen, B.P., Northen, T.R., 2018. Linking soil biology and chemistry in biological soil crust using isolate exometabolomics. Nat. Commun. 9 (1), 19. https://doi.org/10.1038/s41467-017-02356-9.

Tamm, A., Caesar, J., Kunz, N., Colesie, C., Reichenberger, H., Weber, B., 2018. Ecophysiological properties of three biological soil crust types and their photoautotrophs from the succulent Karoo. South Africa. Plant Soil 429 (1), 127–146. https://doi.org/10.1007/s11104-018-3635-4.

Thomas, S., Gaiser, E.E., Gantar, M., Scinto, L.J., 2006. Quantifying the responses of calcareous periphyton crusts to rehydration: a microcosm study (Florida Everglades). Aquat. Bot. 84 (4), 317–323. https://doi.org/10.1016/j.aquabot.2005.12.003.

Venter, A., Siebert, S., Rajakaruna, N., Barnard, S., Levanets, A., Ismail, A., Allam, M., Peterson, B., Sanko, T., 2018. Biological crusts of serpentine and non-serpentine soils from the Barberton Greenstone Belt of South Africa. Ecol. Res. 33 (3), 629–640. https://doi.org/10.1007/s11284-017-1546-0.

Wang, G., Yuan, Y., Morel, J.L., Feng, Z., Chen, D., Lu, C., Guo, M., Liu, C., Wang, S., Chao, Y., Tang, Y., Zhao, D., Xiao, S., Zhang, W., Qiu, R., 2020a. Biological aqua crust mitigates metal(loid) pollution and the underlying immobilization mechanisms. Water Res. 190, 116736. https://doi.org/10.1016/j.watres.2020.116736.

Wang, G., Zhao, W., Yuan, Y., Morel, J.L., Chi, H., Feng, W., Wang, S., Zhang, J., Feng, Z., Tan, H., Chen, D., Ding, W., Liu, C., Qiu, R., 2020b. Mobility of metal(loid)s in Pb/Zn tailings under different revegetation strategies. J. Environ. Manage. 263, 110323 https://doi.org/10.1016/j.jenvman.2020.110323.

Wang, G., Yin, X., Feng, Z., Chen, C., Chen, D., Wu, B., Liu, C., Morel, J.L., Jiang, Y., Yu, H., He, H., Chao, Y., Tang, Y., Qiu, R., Wang, S., 2023. Novel biological aqua crust enhances in situ metal(loid) bioremediation driven by phototrophic/diazotrophic biofilm. Microbiome 11 (1), 110. https://doi.org/10.1186/s40168-023-01549-3.

Wang, G., Feng, Z., Yin, X., Chen, D., Zhao, N., Yuan, Y., Chen, C., Liu, C., Ao, M., Chen, L., Chen, Z., Yang, W., Li, D., Morel, J.L., Chao, Y., Wang, P., Tang, Y., Qiu, R., Wang, S., 2024. Biogenic manganese oxides promote metal(loid) remediation by shaping microbial communities in biological aqua crust. Water Res. 253, 121287 https://doi.org/10.1016/j.watres.2024.121287.

Wang, L., Li, J., Zhang, S., 2022a. A comprehensive network integrating signature microbes and crucial soil properties during early biological soil crust formation on tropical reef islands. Front. Microbiol. 13 https://doi.org/10.3389/fmicb.2022.831710.

Wang, Y., Tang, Y., Yuan, Z., 2022b. Improving food waste composting efficiency with mature compost addition. Bioresour. Technol. 349, 126830 https://doi.org/10.1016/j.biortech.2022.126830.

Weber, B., Wu, D., Tamm, A., Ruckteschler, N., Rodríguez-Caballero, E., Steinkamp, J., Meusel, H., Elbert, W., Behrendt, T., Sörgel, M., Cheng, Y., Crutzen, P.J., Su, H., Pöschl, U., 2015. Biological soil crusts accelerate the nitrogen cycle through large NO and HONO emissions in drylands. Proc. Natl. Acad. Sci. USA 112 (50), 15384–15389. https://doi.org/10.1073/pnas.151581811.

Weber, B., Bowker, M., Zhang, Y., Belnap, J., 2016. Natural recovery of biological soil crusts after disturbance. In: Weber, B., Büdel, B., Belnap, J. (Eds.), Biological Soil Crusts: an Organizing Principle in Drylands. Springer International Publishing, Cham, pp. 479–498. https://doi.org/10.1007/978-3-319-30214-0_23.

Weber, B., Belnap, J., Büdel, B., Antoninka, A.J., Barger, N.N., Chaudhary, V.B., Darrouzet-Nardi, A., Eldridge, D.J., Faist, A.M., Ferrenberg, S., Havrilla, C.A., Huber-Sannwald, E., Malam Issa, O., Maestre, F.T., Reed, S.C., Rodriguez-Caballero, E., Tucker, C., Young, K.E., Zhang, Y., Zhao, Y., Zhou, X., Bowker, M.A., 2022. What is a biocrust? a refined, contemporary definition for a broadening research community. Biol. Rev. 97 (5), 1768–1785. https://doi.org/10.1111/brv.12862.

Witzgall, K., Vidal, A., Schubert, D.I., Höschen, C., Schweizer, S.A., Buegger, F., Pouteau, V., Chenu, C., Mueller, C.W., 2021. Particulate organic matter as a functional soil component for persistent soil organic carbon. Nat. Commun. 12 (1), 4115. https://doi.org/10.1038/s41467-021-24192-8.

Xiao, J., Lan, S., Zhang, Z., Yang, L., Qian, L., Xia, L., Song, S., Farías, M.E., Torres, R.M., Wu, L., 2022. Physical disturbance reduces cyanobacterial relative abundance and substrate metabolism potential of biological soil crusts on a gold mine tailing of Central China. Front. Microbiol. 13 https://doi.org/10.3389/fmicb.2022.811039.

Xu, M., Cui, Y., Beiyuan, J., Wang, X., Duan, C., Fang, L., 2021. Heavy metal pollution increases soil microbial carbon limitation: evidence from ecological enzyme stoichiometry. Soil Ecol. Lett. 3 (3), 230–241. https://doi.org/10.1007/s42832-021-0094-2.

Yang, H., Liu, L., Li, X., Wei, Y., Li, X., Jia, R., 2014. Water repellency of biological soil crusts and influencing factors on the southeast fringe of the Tengger Desert, north-Central China. Soil Sci. 179 (9) https://doi.org/10.1097/SS.0000000000000084.

Ye, Z.H., Shu, W.S., Zhang, Z.Q., Lan, C.Y., Wong, M.H., 2002. Evaluation of major constraints to revegetation of lead/zinc mine tailings using bioassay techniques. Chemosphere 47 (10), 1103–1111. https://doi.org/10.1016/S0045-6535(02)00054-1.

Yilmaz, P., Parfrey, L.W., Yarza, P., Gerken, J., Pruesse, E., Quast, C., Schweer, T., Peplies, J., Ludwig, W., Glöckner, F.O., 2014. The SILVA and "all-species living tree project (LTP)" taxonomic frameworks. Nucleic Acids Res. 42 (D1), D643–D648. https://doi.org/10.1093/nar/gkt1209.

You, X., Xu, N., Yang, X., Sun, W., 2021. Pollutants affect algae-bacteria interactions: a critical review. Environ. Pollut. 276, 116723 https://doi.org/10.1016/j.envpol.2021.116723.

Yuan, M.M., Guo, X., Wu, L., Zhang, Y., Xiao, N., Ning, D., Shi, Z., Zhou, X., Wu, L., Yang, Y., Tiedje, J.M., Zhou, J., 2021a. Climate warming enhances microbial network complexity and stability. Nat. Clim. Chang. 11 (4), 343–348. https://doi.org/10.1038/s41558-021-00989-9.

Yuan, S., Xu, R., Wang, D., Lin, Q., Zhou, S., Lin, J., Xia, L., Fu, Y., Gan, Z., Meng, F., 2021b. Ecological linkages between a biofilm ecosystem and reactor performance: the specificity of biofilm development phases. Environ. Sci. Technol. 55 (17), 11948–11960. https://doi.org/10.1021/acs.est.1c02486.

Zhang, Y.M., Wang, H.L., Wang, X.Q., Yang, W.K., Zhang, D.Y., 2006. The microstructure of microbiotic crust and its influence on wind erosion for a sandy soil surface in the Gurbantunggut Desert of northwestern China. Geoderma 132 (3), 441–449. https://doi.org/10.1016/j.geoderma.2005.06.008.

Zhao, C., Zheng, R., Shi, X., Wang, L., 2021. Soil microbes and seed mucilage promote growth of the desert ephemeral plant *Nepeta micrantha* under different water conditions. Flora 280, 151845. https://doi.org/10.1016/j.flora.2021.151845.

Zhou, J., Deng, Y., Luo, F., He, Z., Tu, Q., Zhi, X., 2010. Functional Molecular Ecological Networks. Mbio 1 (4), e00169-110. https://doi.org/10.1128/mBio.00169-10.

Zhou, J., Deng, Y., Luo, F., He, Z., Yang, Y., 2011. Phylogenetic molecular ecological network of soil microbial communities in response to elevated CO2. MBio 2 (4), e00122-00111. https://doi.org/10.1128/mBio.00122-11.